HAL
open science

Insights into the Crystal Structure and Clathration Selectivity of Organic Clathrates Formed with Hydroquinone and (CO2 + CH4) Gas Mixtures

Jean-Philippe Torré, Heinz Gornitzka, Romuald Coupan, Christophe Dicharry, Martín Pérez-Rodríguez, Antonio Comesaña, Manuel M. Piñeiro

To cite this version:

Jean-Philippe Torré, Heinz Gornitzka, Romuald Coupan, Christophe Dicharry, Martín Pérez-Rodríguez, et al.. Insights into the Crystal Structure and Clathration Selectivity of Organic Clathrates Formed with Hydroquinone and (CO2 + CH4) Gas Mixtures. Journal of Physical Chemistry C, 2019, 123 (23), pp.14582-14590. 10.1021/acs.jpcc.9b04081 . hal-02279913

HAL Id: hal-02279913

https://hal.science/hal-02279913v1

Submitted on 5 Sep 2019

HAL is a multi-disciplinary open access archive for the deposit and dissemination of scientific research documents, whether they are published or not. The documents may come from teaching and research institutions in France or abroad, or from public or private research centers.

L'archive ouverte pluridisciplinaire **HAL**, est destinée au dépôt et à la diffusion de documents scientifiques de niveau recherche, publiés ou non, émanant des établissements d'enseignement et de recherche français ou étrangers, des laboratoires publics ou privés.

Open Archive Toulouse Archive Ouverte

OATAO is an open access repository that collects the work of Toulouse researchers and makes it freely available over the web where possible

This is an author's version published in: http://oatao.univ-toulouse.fr/24197

Official URL: https://doi.org/10.1021/acs.jpcc.9b04081

To cite this version:

Torré, Jean-Philippe and Gornitzka, Heinz and Coupan, Romuald and Dicharry, Christophe and Pérez-Rodríguez, Martín and Comesaña, Antonio and Piñeiro, Manuel M. *Insights into the Crystal Structure and Clathration Selectivity of Organic Clathrates Formed with Hydroquinone and (CO2 + CH4) Gas Mixtures.* (2019) The Journal of Physical Chemistry C, 123 (23). 14582-14590. ISSN 1932-7447

Any correspondence concerning this service should be sent to the repository administrator: tech-oatao@listes-diff.inp-toulouse.fr

Insights into the Crystal Structure and Clathration Selectivity of Organic Clathrates Formed with Hydroquinone and (CO_2 + CH_4) Gas Mixtures

Jean-Philippe Torré,[*,†] Heinz Gornitzka,[‡] Romuald Coupan,[§] Christophe Dicharry,[∥] Martín Pérez-Rodríguez,[⊥] Antonio Comesaña,[⊥] and Manuel M. Piñeiro[⊥]

[†]Laboratoire de Génie Chimique, Université de Toulouse, CNRS, INPT, UPS, 31000 Toulouse, France

[‡]Laboratoire de Chimie de Coordination LCC-CNRS, Université de Toulouse, CNRS, UPS, 31400 Toulouse, France

[§]Total Research & Technology Feluy, Zone Industrielle Feluy C, B-7181 Seneffe, Belgium

[∥]CNRS/TOTAL/UNIV PAU & PAYS ADOUR/E2S UPPA, Laboratoire des Fluides Complexes et leurs Réservoirs-IPRA, UMR5150—avenue de l'Université, 64000 Pau, France

[⊥]Departamento de Física Aplicada, Facultade de Ciencias, Universidade de Vigo, 36310 Vigo, Spain

ABSTRACT: Organic clathrates, particularly those formed by hydroquinone (HQ) and gas mixtures, have been far less studied than other inclusion compounds, such as gas hydrates. In this study, experiments and molecular dynamics simulations were performed on mixed (CO_2 + CH_4)−HQ clathrates. Single crystals were synthesized using gas mixtures with different compositions, ranging from pure CO_2 to pure CH_4. The crystal structure, the guest occupancy in the clathrates, and the variation of the crystal lattice parameters according to clathrate composition were obtained by X-ray diffraction measurements. In addition, molecular dynamics simulations were performed on the same systems, with state-of-the-art molecular models and force fields. The experimental results obtained and the molecular dynamics simulation estimations were in good agreement. The clathration selectivity was also calculated on the basis of experimental results, and the composition of the solid phase was correlated with the composition of the gas phase at equilibrium. These new insights into these structures will be useful from both a fundamental and a practical point of view, particularly for further developing innovative gas separation techniques using HQ clathrates.

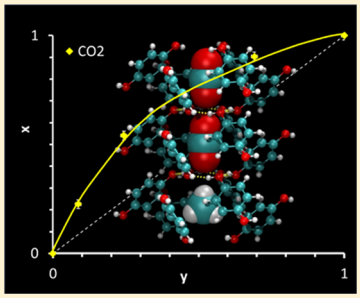

INTRODUCTION

The term "clathrate" refers to a solid-state supramolecular entity composed of a network of self-associating molecules (called hosts) forming cavities or channels in which other species (called guests) can be encaged.[1] These host−guest complexes crystallize if the size of the cavities is compatible with the size and shape of the guests, but only under specific thermodynamic (i.e., temperature and pressure) conditions, and they are generally unstable if the cavities do not contain a certain fraction of guest molecules. Clathrate hydrates (usually known as gas hydrates or simply hydrates) represent the most studied category of clathrate compounds,[2] particularly natural gas hydrates that have been known for their propensity to plug the flowlines used in oil and gas transportation.[3] Clathrates whose framework is entirely made up of organic molecules are called organic clathrates. These compounds, particularly those formed with hydroquinone (HQ), have been far less studied than the well-known gas hydrates.

Hydroquinone (1,4 dihydroxybenzene, formerly referred to as quinol) is able to form organic clathrates by encaging gaseous guest molecules such as methane (CH_4), carbon dioxide (CO_2), sulfur dioxide (SO_2), hydrogen sulfide (H_2S) among others.[4] The general formula of HQ clathrates is χG-$3C_6H_4(OH)_2$, where G stands for the encaged guest species and χ is the occupancy factor (i.e., the fraction of cavities that are occupied). Note that the value of χ might theoretically vary from 0 for a guest-free clathrate (if all of the cavities are empty) to 1 (if all of the cavities are fully occupied).

HQ clathrates (denoted by β-HQ), discovered more than 150 years ago[5] and considered for ages as just a fascinating scientific oddity, actually have very interesting properties: (i) these crystals can store large quantities of gases;[6] (ii) can release (or absorb) energy when the guests enter (or exit) the clathrate structure;[7] in the case of some systems, (iii) have a very high stability at ambient conditions that is ideal for applying analytical characterization techniques;[8] and (iv) can exist in a metastable state with no guests present in the lattice structure.[9,10] As a result, practical applications based on HQ clathrates have been proposed, including sequestration of hazardous substances,[11] fractionation of organic compound

DOI: 10.1021/acs.jpcc.9b04081

mixtures,[12] hydrogen storage,[13,14] and separation of CO_2 from different gas mixtures containing H_2,[15] N_2,[16] and CH_4.[1717]

In the late 1940s, Powell was the first ever to resolve an organic clathrate structure (HQ−SO_2) by X-ray crystallographic analysis, revealing one of the key elements for understanding the nature of these compounds.[18] However, more than 75 years on, it is amazing to realize just how many simple and basic organic clathrate systems still remain unexplored, particularly among those formed with gases.[19,20] For example, the detailed molecular structures of HQ−CH_4 and mixed (CH_4−CO_2)−HQ clathrates have still not been published. Indeed, this area has not yet been thoroughly studied and HQ clathrates could open up interesting new scientific avenues for exploration.

When different guests are encaged in an HQ structure (typically when a gas mixture is used instead of a pure gas), the resulting host−guest compounds are known as "mixed gas HQ clathrates".[21] Mixed gas clathrates could be used in a number of practical applications such as gas separation by selective clathration. However, there is very little fundamental information on mixed gas HQ clathrates in the literature, except for recent physicochemical characterizations, and in spectroscopic and thermodynamic data.[9,22−24] From a crystallographic point of view, even less information is available. Lee et al. studied the properties of (C_2H_4−CH_4)−HQ and (C_2H_4−C_2H_6)−HQ clathrates and found that the lattice parameters *a*, *b*, and *c* (calculated from X-ray powder diffraction patterns) generally increase with the concentration of C_2H_4 in the gas phase.[25,26] However, to the best of the author's knowledge, no detailed crystal structures of the kind organic clathrates form with gas mixtures have ever been reported.

Molecular dynamics (MD) simulations of clathrates have been described in the literature, although there are not as many of them as one might expect, considering the abundance and availability of certain host molecules such as water or HQ. Among the clathrates, gas hydrates are by far the systems that receive the most attention in simulation studies. Several reviews, those of Sum et al.[27] and Barnes and Sum,[28] for example, offer detailed theoretical descriptions of their thermophysical properties and equilibrium phenomena simulated by MD. HQ clathrates have received far less attention in molecular dynamics studies, although they share many structural features with hydrate clathrates. To our knowledge, the first study was presented by Dang and Pettitt,[29] in which they investigated the thermodynamics and guest dynamics of krypton (Kr) and argon (Ar) HQ clathrates.[30] This study was promptly followed by a second one by the same authors on diatomic molecules. Santikary et al.[31] studied the diffusion of noble gases (neon and argon) through rigid HQ lattices. Daschbach et al.[32] and more recently Pérez-Rodríguez et al.[33] investigated the behavior of H_2 as a guest molecule, whereas Nemkevich et al.[34] studied HQ clathrates with Dianin's compound. Other guests including CO_2, CO, H_2S, and CH_4 were also previously modeled by Zubkus et al.[35,36] Recently, a study of HQ clathrates with CH_4 and CO_2 as guest molecules was presented,[37] in which only the clathrates of the two guests in their pure state (not their mixtures) were investigated. In this study, a molecular dynamics model based in an optimized potentials for liquid simulations (OPLS) force field was tested and the solid native α phase and the β clathrate phases of HQ with CH_4 and CO_2 as guest molecules were reproduced with reasonable accuracy.

In the present study, we investigated the crystal structure of mixed (CO_2 + CH_4)−HQ clathrates in a combined experimental and numerical approach. Single crystals were synthesized using CO_2/CH_4 gas mixtures with different compositions ranging from pure CO_2 to pure CH_4, and the crystal structure was resolved using X-ray diffraction (XRD). The main objective was to study how the lattice parameters of these mixed gas clathrates vary according to the proportion of CO_2 and CH_4 loaded in the crystal. The selectivity of the clathration (i.e., the capacity of the crystal to selectively encapsulate one of the two molecules present in the gas mixture used to form it) was also analyzed experimentally across the entire gas composition domain. In parallel, molecular dynamics simulations were performed on the same systems using state-of-the-art molecular models and force fields, namely, solving Newton's equations of motion for the individual atoms, coupled with a barostat and a thermostat to fix their thermodynamic conditions at the thermodynamic points of interest. Finally, the experimental and numerical results obtained were compared and discussed to offer salient conclusions regarding the structure and composition of these mixed gas organic clathrates.

■ EXPERIMENTAL SECTION

The gas clathrates are crystallized in a 168.0 ± 0.9 cm^3 high-pressure jacketed reactor equipped with two viewing windows to watch the crystals growing during the experiment, two Pt-100 probes to measure the liquid and gas temperatures with an accuracy of ± 0.1 K, and a Keller pressure sensor (accuracy of ± 0.01 MPa). The protocol used here was previously used in another of the authors' studies to obtain CO_2−HQ clathrate single crystals.[8] In short, an oversaturated solution of HQ in absolute ethanol (EtOH),[38] typically 8 g of HQ in 11 g of EtOH, is first prepared in a small glass vessel containing a star-shaped magnetic stirring bar. This vessel is placed inside the reactor in front of the viewing windows with the help of a clamp. The reactor is then closed, put under vacuum to eliminate any traces of air, and regulated to a temperature of 298 ± 0.1 K. The initial HQ/EtOH suspension is agitated with a magnetic stirrer situated beneath the reactor to properly dissolve the HQ and saturate the solvent. The agitation is stopped to perform the next operations in quiescent conditions. The reactor is pressurized either with pure CO_2 (or CH_4) or with a CO_2−CH_4 gas mixture until the desired pressure of 3.0 MPa is reached. The temperature and pressure used in this work were chosen based on previous studies by the authors, particularly two: the first is a process evaluation of CO_2/CH_4 separation by HQ clathrate formation in which a temperature of 298 K and a pressure of 3.0 MPa could be a relevant operating point for an industrial production gas separation unit using such a technology;[17] the second presents a wide range of physical and chemical characterization results for (CO_2−CH_4)−HQ clathrates obtained at ambient conditions and 3.0 MPa but did not study crystal structures.[24] Both temperature and pressure are maintained constant during crystallization. The crystals inside the reactor are observed using a commercial webcam (LiveCam Optia AF, Creative Labs), and all of the process data (i.e., pressure and temperature versus time) are recorded using a homemade LabVIEW interface with an acquisition frequency of 1 Hz. At the end of the synthesis, the composition of the gas mixture at equilibrium with the clathrates is analyzed by gas chromatography (GC). The reactor is then isolated (i.e., the gas supply

DOI: 10.1021/acs.jpcc.9b04081

valve is closed) and transported (under pressure) to the analytical room for XRD analysis. It is depressurized and opened to collect the clathrate crystals, and the XRD analysis is performed immediately at 100 K. Technical details on GC, XRD apparatus and methods, and information about the equipment used in this work are summarized in Tables S1 and S2 of the Supporting Information. Figures showing the crystal structure and the voids were obtained using Mercury 3.10.3.[39]

NUMERICAL METHODS

For simulating the mixed gas HQ clathrate, we use a molecular dynamics technique based on molecular models and a methodology previously tested for pure CO_2 and CH_4 HQ clathrates.[37] GROMACS software[40,41] is used to carry out all MD simulations in the present work.

The initial coordinates of the HQ lattice are obtained from experimental crystallographic data acquired by X-ray diffraction analysis.[8] The simulation boxes for the β-HQ clathrates are shown in Figure 1. The initial cell parameters of β-HQ are taken from the experimental values $a = b = 1620.7 \pm 0.6$ pm, $c = 578.0 \pm 0.2$ pm. We fill the β-HQ lattice with different concentrations of CO_2 and CH_4, and each system is then equilibrated at the desired temperature and pressure values. We select the OPLS-all atom (AA)[42] force field, somewhat modified for modeling the HQ lattice and guest molecules. In the model used here, the C6 rings in the HQ molecules are rigid, as are the CO_2 and CH_4 guest molecules, but the OH moieties have some freedom to rotate. All of the molecules are supposed to be nonpolarizable, meaning that the atoms are modeled as point particles with fixed relative positions and point charges.

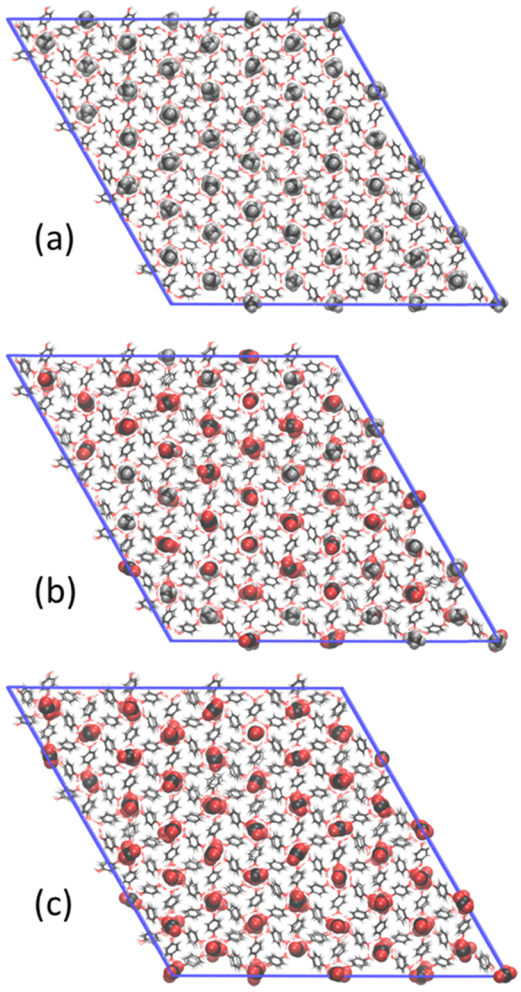

Figure 1. Snapshot of the rhombohedral simulation boxes for the β-HQ clathrate, containing as guest molecules (a) CH_4, (b) an equimolar concentration of CO_2 and CH_4, and (c) CO_2. The views were taken along the z-axis, so the clathrate channels are perpendicular to the page plane. Each channel, consisting, for this system size, four aligned cells, shows the superimposition of all of the guest molecules it contains.

The modifications made to the OPLS-AA force field used in this study concern the atomic equilibrium positions and charges recalculated from quantum mechanics (QM) instead of the default values in the force field tables. To ensure compatibility with the original OPLS-AA parameterization scheme, equilibrium geometries of HQ, CO_2, and CH_4 are obtained using Becke's three-parameter hybrid functional B3LYP (Becke, Lee−Yang−Parr)[43,44] with the 6-31+G(d,p) Pople basis set implemented in Gaussian 09.[45] Atomic point charges are recalculated with the help of the CHELPG scheme developed by Breneman and Wiberg[46] in Gaussian 09 too.

The initial simulation boxes are prepared (optimized and equilibrated) in the canonical (NVT) ensemble, coupled with the thermostat by Bussi et al.[47] When the simulation boxes are stabilized, we calculate the lattice parameters of the mixed gas HQ clathrate crystal structures by performing independent simulations with different relative concentrations of guest molecules in the isothermal−isobaric (NpT) ensemble. The pressure is stabilized at selected values by means of the Parrinello−Rahman barostat[47] using anisotropic compressibility to take into account the rhombohedral symmetry of the HQ clathrate crystal. As usual, three-dimensional (3D) periodic boundary conditions are used in conjunction with the minimum image convention. The interaction potentials are truncated so that the explicit interactions remain inside the simulation box. Cutoff values of 110 pm are used for both the Lennard-Jones and Coulombic potentials. To evaluate these interactions, we chose the fourth-order particle mesh Ewald method[48,49] with a ratio mesh of 120 pm. To describe cross interactions, we use the Lorentz−Berthelot combining rules with a geometric mean.[50]

RESULTS AND DISCUSSION

A summary of the experimental results obtained in this study is given in Table S3 of the Supporting Information, including CO_2 molar fraction in the gas phase in equilibrium with the solid phase measured at the end of the experiment, A and B parameters of the clathrate formula, crystal lattice parameters (a, b, c), tilt angle of the HQ molecule in the crystal (α), volume of the unit cell (V_{uc}), total occupancy of the guests in the clathrate (χ), CO_2 molar fraction in the crystal (x^{CO_2}), ratio of the CO_2 and CH_4 molar fractions in the crystal (S^{CO_2/CH_4}), and separation factor (SF^{CO_2/CH_4}).

Crystal Structure. The modeled crystal structure is shown in Figure 2. Figure 3a−c shows general views of the host crystal structure for the mixed (CO_2 + CH_4)−HQ clathrates obtained experimentally. The global rhombohedral structure (symmetry group $R\bar{3}$) is the same whether the clathrates are obtained with mixed or pure gases (i.e., CO_2 and CH_4). The geometry is based on the formation of two interpenetrating, but not interconnected, networks of HQ molecules forming a cavity in which the guest molecules are encapsulated. The hydroxyl

DOI: 10.1021/acs.jpcc.9b04081

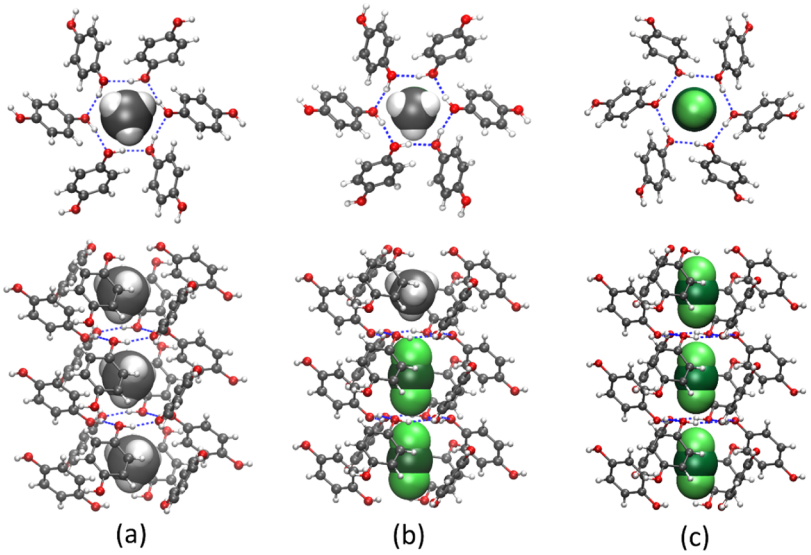

Figure 2. Detailed view of the molecular dynamics simulation structure for the β-HQ clathrates, showing only three consecutive cells of a given channel. (a) Channel containing CH_4 as a guest molecule, (b) channel containing CO_2 + CH_4, and (c) channel containing CO_2. In each case, a vertical (along the *z*-axis) and a side (along the *x*-axis) view are presented.

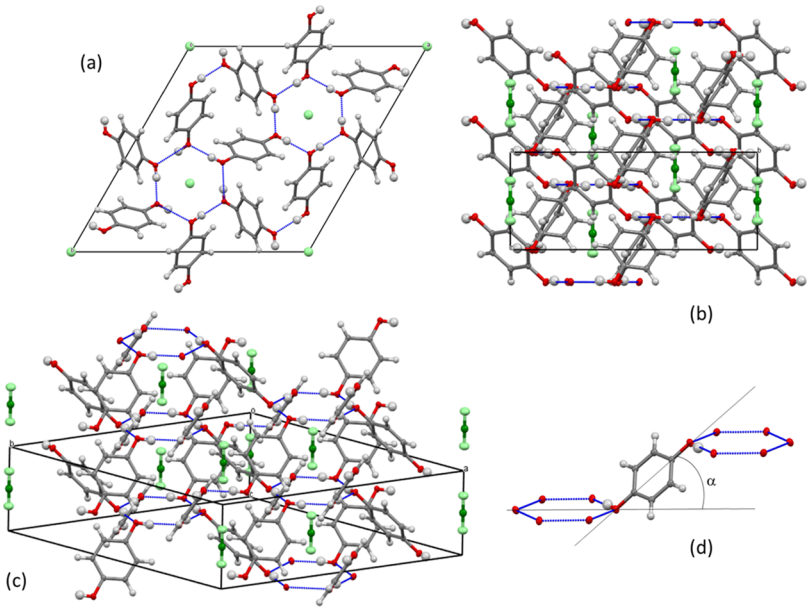

Figure 3. General views of the crystal structure of mixed (CO_2−CH_4)−HQ clathrates obtained experimentally: (a) view down the crystallographic *c*-axis; (b) view down the crystallographic *a*-axis; and (c) 3D view. Blue dotted lines are hydrogen bonds forming the planar hexagons at the top and bottom of the cavity. (d) HQ molecule is represented with its oxygen−oxygen axis tilted at an angle α to the *c* plane (0001). The structures presented in this figure were built with the clathrate ($0.59CO_2$−$0.23CH_4$)−3HQ (CDCC-1913200).

groups of HQ are linked by hydrogen bonding and form a planar hexagon defining the top and bottom of this cavity, whereas alternate HQ molecules pointing diagonally above and below each hexagon define the lateral parts of the cavity. Interestingly enough, we found that all of the clathrates analyzed in this study have the same crystallographic structure. The lattice parameters, however, strongly depend on the composition of the gas loaded into the clathrates, as discussed later on. In addition to the lattice parameters, the α angle (tilt angle of the O−O HQ molecule axis in relation to the *c* plane) shown in Figure 3d also characterizes the structure. In an attempt to get a better idea of the cavity shape, Figure 4 shows the voids present in the crystal, focusing on the solvent-accessible surface areas. With this approximation, the crystal is considered as a set of fused spheres with van der Waals radii. A probe sphere (of a defined radius) is then rolled over the van der Waals surface, and the accessible surface is mapped out by the center of the probe sphere to obtain a 3D view of the voids in the crystal.[51] This method has already been used to characterize various materials such as salycilamide polymorphs,[52] L-alanyl-L-valine,[53] gabapentin heptahydrate,[54] and adamantane hydrochloride salts.[55] The HQ clathrate cavity exhibits a roughly spherical shape with pure CH_4 (see Figure 4a), whereas it is largely elongated toward the *c*-axis in the case of pure CO_2 (see Figure 4b). Interestingly enough, the cavity shape of the mixed (CO_2−CH_4)−HQ clathrates is halfway

DOI: 10.1021/acs.jpcc.9b04081

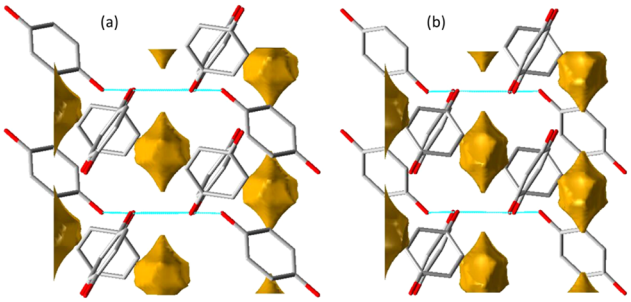

Figure 4. Representations of typical cavities in HQ clathrates (down the crystallographic *a*-axis) obtained from a crystal structure analysis by XRD. The "solvent-accessible voids" are visualized using a probe sphere of 1.2 Å and a grid spacing of 0.2 Å. (a) CH_4−HQ clathrate. (b) CO_2−HQ clathrate.

between those obtained with pure gases: the more CO_2 enclathrated in the cavity, the more deformed it is.

As both CO_2 and CH_4 are enclathrated, the formula of the mixed (CO_2 + CH_4) clathrate can be written as:

$(ACO_2 + BCH_4)\cdot 3HQ$, with $A + B = \chi$ with $(0 \leq \chi \leq 1)$ and where A and B are defined as the CO_2 and CH_4 occupancy factors, respectively. These factors can be normalized by the global occupancy χ to give normalized occupancy factors $x^{CO_2} = A/\chi$ and $x^{CH_4} = B/\chi$. The values x^{CO_2} and x^{CH_4} are the molar fractions of the CO_2 and CH_4 trapped inside the clathrate. The composition of the clathrate was calculated by structural analysis. For this purpose, the carbon and oxygen atom occupancies in the guest molecules were refined separately using two different variables. Given that the carbon atoms of both guest molecules are located in the same position, the variable for carbon atom occupancy gives the total occupancy of the guest molecules. The value of the oxygen atom variable reflects the CO_2 occupancy and the difference between the two variables gives the information pertaining to the CH_4 molecules. It has been proven that this technique gives occupancy values of the same order of magnitude as those obtained by TGA measurements.[8] In this work, the occupancies and clathrate formulas determined by XRD analysis were crosschecked by elementary analysis. In addition, the reproducibility of the experiments, estimated based on three independent runs carried out in the same conditions using an initial 50:50 CO_2/CH_4 gas mixture, is quite good as the average results obtained by structural analysis were A = 0.57 ± 0.03 and B = 0.22 ± 0.03 against A = 0.52 ± 0.12 and B = 0.19 ± 0.07 by elementary analysis.

The experimental values of parameters A and B of the clathrate formula $(ACO_2 + BCH_4)\cdot 3HQ$ are plotted in Figure 5 versus the molar fraction of CO_2 in the gas phase in equilibrium with the crystal. It is therefore very simple using these curves to obtain the clathrate formula for a given gas composition at 298 K and 3 MPa. Interestingly enough, both the crystal lattice parameters, i.e., a (=b) and c, obtained experimentally and by modeling appear to be directly correlated with the clathrate composition. The variation of the lattice parameters and the angle α versus x^{CO_2} are shown in Figures 6 and 7, respectively. Note that as $x^{CH_4} = 1 - x^{CO_2}$, the variation of the lattice parameters versus x^{CH_4} can be deduced very easily.

When the clathrate became increasingly rich in CO_2, we observed both a decrease in the a (= b) lattice parameter and an increase in the c parameter: the size of the unit cell is

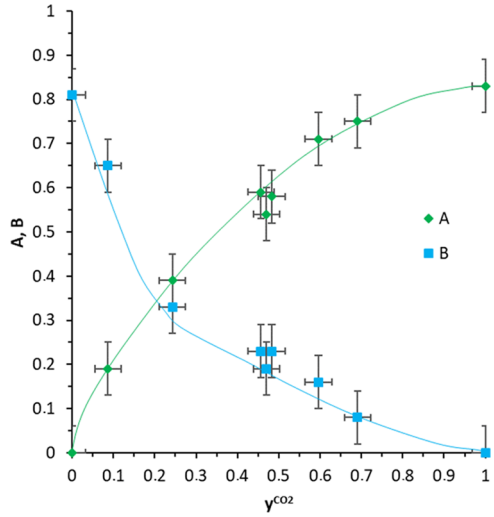

Figure 5. Variation of A and B (parameters of the clathrate formula $(ACO_2 + BCH_4)\cdot 3HQ$) as a function of the molar fraction of CO_2 in the gas phase at equilibrium with the crystal. Experimental data were obtained with clathrates synthesized at T = 298 K and P = 3.0 MPa and analyzed with XRD at T = 100 K and P = 0.1 MPa. The blue and green lines are guides for the eye.

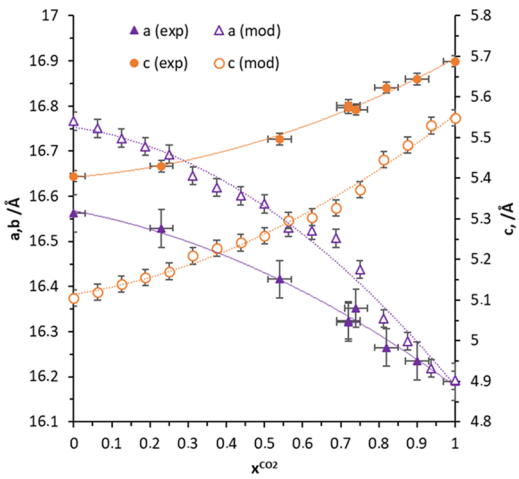

Figure 6. Variation of the lattice parameters of the (CO_2 + CH_4)−HQ clathrate crystals as a function of the molar fraction of CO_2 in the solid phase. Experimental data were obtained with clathrates synthesized at T = 298 K and P = 3.0 MPa and analyzed with XRD at T = 100 K and P = 0.1 MPa. Modeling data were obtained at T = 100 K and P = 0.1 MPa. The orange and purple lines are guides for the eye.

therefore strongly dependent on the composition of the gas encapsulated in the clathrate. With this particular binary gas mixture and in these conditions, the variation of the lattice parameters is monotonous (no extremum found). This trend clearly demonstrates that the HQ framework is highly adaptive.

We observed that MD estimates almost systematically deviate from experimental values, but, despite this, the performance of the HQ molecular model and the force field used can be considered quantitatively good. Let us recall that the HQ force field used combines two different approaches. First, the dispersive interaction parameters were originally computed in a group contribution scheme for substituted benzene derivatives in the OPLS force field. It is important to note that dispersive characteristic parameters are adjusted to

DOI: 10.1021/acs.jpcc.9b04081

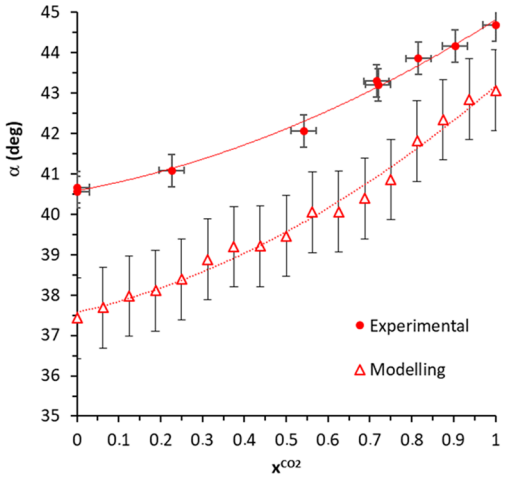

Figure 7. Variation of the α angle (tilt angle of the HQ molecule axis in relation to the c plane) as a function of the molar fraction of CO_2 in the solid phase. Experimental data were obtained with clathrates synthesized at T = 298 K and P = 3.0 MPa and analyzed with XRD at T = 100 K and P = 0.1 MPa. Modeling data were obtained at T = 100 K and P = 0.1 MPa. The red lines are guides for the eye.

reproduce experimental fluid-phase equilibrium data. The same applies for CO_2 and CH_4 force fields. The original HQ molecular model was then modified by recalculating the atomic point electric charges using QM calculations for an isolated molecule under vacuum. This means that the force field characteristic parameters were determined in conditions far removed from those studied for the present clathrates, underlining the remarkable transferability of force field parameters. The geometry of the HQ clathrate containing a single guest was found to be very similar to the results obtained in experiments,[37] an encouraging first result. Because we are able to demonstrate that the clathrate structure is flexible enough to accommodate a mixed population of guest molecules, in keeping with the trend highlighted in experiments concerning the variation of a and c lattice parameters, these simulation results can be considered highly relevant in light of the hypotheses and simplifications used in the models (conventional, nonpolarizable, etc.). There was a certain drift in the estimated results, but the structural modification undergone by the clathrate with the change in guest composition is extremely subtle in experiments, and the simulations were able to very accurately capture this physical behavior.

Drawing on the analysis of the molecular dynamics simulation results, the shape of the clathrate cavities of the mixed clathrates can also be discussed. In the case of pure guest (CH_4 or CO_2) HQ clathrates, it is clear that all cavities have the same geometry, with a given set of lattice parameter values, regardless of the fluctuations in cage size due to the movement of the HQ molecules, which are bonded by labile hydrogen bonds only. Nevertheless, in the case of mixed guest clathrates, there is some controversy about the possible coexistence of clathrate cavities of different sizes for each type of guest molecule. Based on an analysis of the molecular dynamics simulation trajectory, a histogram of the α angle values for the pure CH_4, pure CO_2, and equimolar guest clathrate structures was calculated at 100 K and 0.1 MPa. The data obtained follow a normal distribution (see details of the statistical analysis in Table S4 of the Supporting Information). The results presented in Figure 8 show a clearly monomodal cavity size distribution for the mixed clathrate too, which rules

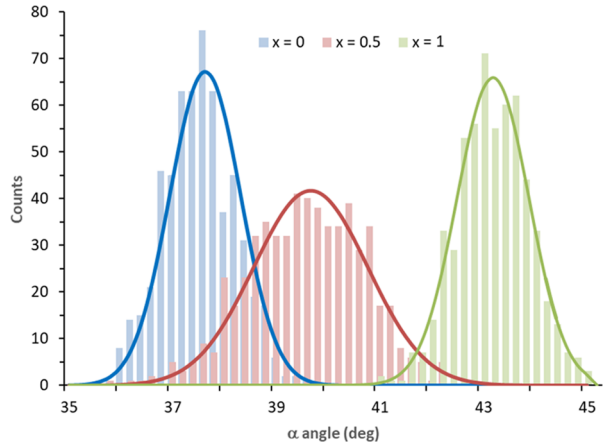

Figure 8. Distribution of the HQ molecule tilt angle (α) in the clathrate structure for three values of CO_2 molar fractions in the solid phase (x): x = 0 in blue (CH_4−3HQ); x = 0.5 in red (0.5CO_2 + 0.5CH_4)−3HQ; x =1 in green (CO_2−3HQ), each computed from 576 data points obtained by molecular dynamics simulations at 100 K and 0.1 MPa. Distribution histograms have been plotted with a class size of 0.2°. The solid curves correspond to the normal distribution calculated from the data points.

out the bimodal cage size distribution hypothesis. Molecular dynamics simulation results also support the case of a homogeneous crystalline structure with lattice parameters evolving continuously between the limiting values corresponding to the pure clathrates. This is an estimation result that might have been expected a priori, taking into consideration the reported flexibility of the hydrogen-bonded network of the clathrate structure, which is able to shrink or swell according to changes in guest occupancy rate or composition.

Clathrate Selectivity. The capacity of a clathrate crystal formed with a binary gas mixture to be more or less selective toward one of the two gases in presence can be discussed with the help of the separation factor (denoted SF),[56] which considers both the composition of the enclathrated gas and the composition of the gas phase in equilibrium with the solid phase. This indicator, commonly used in chemical and process engineering studies to quantify clathrate selectivity toward one of the two gases, is expressed in eq 1 for the CO_2/CH_4 binary mixture as

$$\mathrm{SF}^{CO_2/CH_4} = \frac{x^{CO_2}/(1 - x^{CO_2})}{y^{CO_2}/(1 - y^{CO_2})} \quad (1)$$

where x^{CO_2} and y^{CO_2} are the CO_2 molar compositions of the gas present in the clathrate and in the gas phase in the CO_2/CH_4 gas mixture, respectively. The higher the SF, the better the selective clathration toward CO_2.

The composition of the clathrate itself can be simply assessed by the S^{CO_2/CH_4} ratio of the molar fraction of the two gases (i.e., x^{CO_2} and x^{CH_4}) present in the crystal, defined by eq 2

$$S^{CO_2/CH_4} = \frac{x^{CO_2}}{x^{CH_4}} \quad (2)$$

In our case, it is worth noting that S can also be directly calculated by the ratio of the A and B coefficients in the

DOI: 10.1021/acs.jpcc.9b04081

clathrate formula. Obviously, when $S^{CO_2/CH_4} > 1$, the clathrate has more CO_2 than CH_4.

The correlation curve between the composition of the solid and the gas at equilibrium is shown in Figure 9 for a temperature of 298 K. The corresponding values of S and SF versus the CO_2 concentration in the gas phase at equilibrium are plotted in Figure 10.

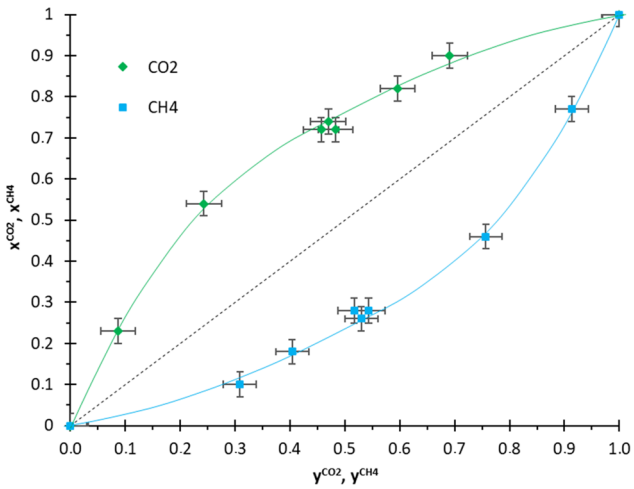

Figure 9. Equilibrium between the CO_2 and CH_4 molar fractions in the HQ clathrate (x^{CO_2} and x^{CH_4}) and the CO_2 and CH_4 molar fractions in the gas phase (y^{CO_2} and y^{CH_4}). The green and blue lines are guides for the eye.

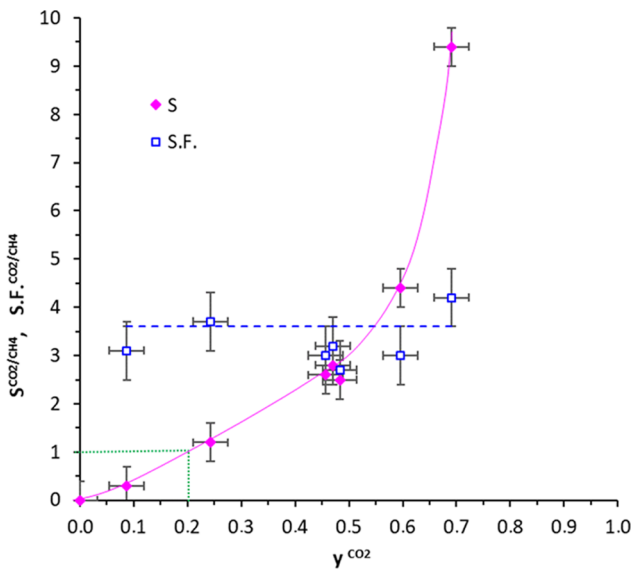

Figure 10. Variation of the ratio of the molar fraction of the CO_2 and CH_4 present in the crystal (S^{CO_2/CH_4}) and of the separation factor (SF) as a function of the molar fraction of CO_2 in the gas phase. The dashed blue line represents the value $SF^{CO_2/CH_4} = 3.6$. The dotted green lines show the value of the CO_2 gas fraction ($y^{CO_2} \sim 0.2$), which corresponds to $S^{CO_2/CH_4} = 1$. The rose line is guide for the eye.

It is clear that in these conditions of synthesis pressure (3.0 MPa), temperature (298 K), and gas mixture composition ($0 < y^{CO_2} < 1$), the x^{CO_2} vs y^{CO_2} curve is always above the diagonal line of this chart (see Figure 9), demonstrating that the molar fraction of CO_2 in the solid phase is always higher than in the gas phase at equilibrium. In other words, the gas that could be recovered by dissociation of the clathrate is always richer in CO_2 than the gas used to form it. Therefore, the HQ clathrates formed from a $CO_2 + CH_4$ gas mixture are selective toward CO_2 for the entire gas composition range. This point is illustrated in Figure 10 by SF^{CO_2/CH_4} values that are greater than 1, i.e., ranging from 2.7 to 4.2.

Actually, the SF values found in this work are different from those previously published in the literature. Coupan et al.[21] calculated SF^{CO_2/CH_4} values lower than 1 across the entire gas composition domain when the clathrate is crystallized from an HQ-saturated solvent solution formed at a very low pressure in conditions of three-phase equilibrium (e.g., $T = 298.3 \pm 0.3$ K, $P = 0.089 \pm 0.013$ MPa, and $y^{CO_2} = 0.512 \pm 0.002$). This comparison might suggest that the clathrate selectivity toward CO_2 becomes much higher than 1 if the clathrate formation pressure largely exceeds the three-phase clathrate equilibrium pressure (in this study, the synthesis pressure is around 30 times higher than the equilibrium pressure). In addition, the SF values in this work were found to be about 3−10 times lower than those obtained by Coupan et al. (i.e., SF^{CO_2/CH_4} from 10.1 to 18.8 at 293 K)[17] and Lee et al.[9] who have also worked with $CO_2 + CH_4$ gas mixtures. These higher SF values could be explained by the fact that the mixed gas HQ clathrates found by Coupan et al. and Lee et al. were obtained (i) through a direct gas−solid reaction instead of crystallization from an HQ-saturated solvent, or (ii) through using an intermediate guest-free HQ clathrate (formed by using CO_2) identified as being particularly selective toward CO_2.[10] However, even though the HQ clathrates were selective toward CO_2 across the entire gas mixture composition domain, it is very interesting to note in Figure 10 that the clathrate crystals contain more CO_2 than CH_4 (i.e., $S^{CO_2/CH_4} > 1$) only when the molar fraction of CO_2 in the gas phase (y^{CO_2}) is higher than around 0.2. We believe that these results could be very useful for practical applications, such as HQ clathrate-based gas separation processes.

■ CONCLUSIONS

Single crystals of mixed ($CO_2 + CH_4$)−HQ clathrates formed with different CO_2/CH_4 gas mixtures were synthesized experimentally and underwent XRD analysis to obtain information on the crystal structures and on the occupancy of the guests enclathrated in the crystal. Molecular dynamics simulations were also performed on the same structures. From the results obtained, it was concluded that mixed ($CO_2 + CH_4$) clathrates have the same rhombohedral crystal structure whatever their composition is (i.e., from pure CO_2 to pure CH_4) and that their homogeneity and concentration depend on cavity size. However, the lattice parameters of the crystal and the size of the cavity vary with the gas mixture composition: when the proportion of CO_2 increases in the crystal, the lattice parameters a and b decrease while c increases, in a monotonic way (without extremum). The more CO_2 there is in the crystal, the more elongated the cavities toward the c-axis. The molecular dynamics simulations very accurately predicted this tendency of the crystal structure to vary according to the gas composition. The lattice parameters obtained in experiments and numerically were in very good agreement, demonstrating that the modeling strategy chosen and the simplified assumptions used are relevant. Interestingly enough, we were able to deduce from the statistical analysis of cavity sizes obtained by simulations, a key aspect of the clathrate structure that is very difficult to process in

DOI: 10.1021/acs.jpcc.9b04081

experiments: even if two different guests are present in the structure (i.e., CO_2 and CH_4) in variable proportions, mixed HQ clathrates have just one cavity size that varies as a function of the composition of the gas encapsulated in the crystal. Calculation of clathrate selectivity demonstrated that, in these conditions (synthesis at a pressure of 3.0 MPa and a temperature of 298 K), HQ clathrates are always selective toward CO_2 whatever the gas composition is:the gas loaded in the clathrates is always richer in CO_2 than the gas used to form it. However, it is worth noting that although the clathration was selective toward CO_2, we found that the clathrates became richer in CH_4 when the CO_2 molar fraction in the gas at equilibrium dropped below ~0.2. We believe that these results concerning clathration selectivity are highly important for practical applications using organic clathrates, particularly CO_2/CH_4 gas separation processes based on HQ clathrates. It could be useful to perform additional work at different pressures and temperatures with this particular gas mixture and others.

■ ASSOCIATED CONTENT

Supporting Information

The Supporting Information is available free of charge on the ACS Publications website at DOI: 10.1021/acs.jpcc.9b04081.

> Analytical techniques, methods and materials used in this study, the snapshot of the rhombohedral simulation boxes for the β-HQ clathrate, the summary of the experimental data obtained, and the statistical analysis of the tilt angle (α) data obtained by simulation (PDF)

Accession Codes

CCDC 1913196−1913204 contain the additional crystallographic data.

■ AUTHOR INFORMATION

Corresponding Author

*E-mail: jean-philippe.torre@ensiacet.fr. Phone: +33(0)5 34 32 37 10.

ORCID

Jean-Philippe Torré: 0000-0001-5735-8626
Christophe Dicharry: 0000-0002-6318-3989
Manuel M. Piñeiro: 0000-0002-3955-3564

Author Contributions

The manuscript was written based on the contributions of all the authors. All of the authors have approved the final version of the manuscript.

Notes

The authors declare no competing financial interest.

■ ACKNOWLEDGMENTS

We would like to acknowledge the CNRS (Centre National de la Recherche Scientifique) for supporting this study. We would also like to thank Joseph Diaz and Mathieu Chabod for their assistance with the experimental apparatus. M.M.P. acknowledges the CESGA (www.cesga.es) for providing access to computing facilities and the Ministerio de Economía y Competitividad in Spain for its financial support [Grant ref FIS2015-68910-P cofinanced by European Regional Development Funds (ERDF)].

■ REFERENCES

(1) Steed, J. W.; Turner, D. R.; Wallace, K. J. *Core Concepts in Supramolecular Chemistry and Nanochemistry*; John Wiley & Sons: Chichester, England, 2007; pp 179−194.

(2) Sloan, E. D.; Koh, C. A. *Clathrate Hydrates of Natural Gases*, 3rd ed.; CRC Press, Taylor & Francis Group: Boca Raton, 2008.

(3) Hammerschmidt, E. F. Formation of Gas Hydrates in Natural Gas Transmission Lines. *Ind. Eng. Chem. Res.* **1934**, *26*, 851−855.

(4) Atwood, J. L.; Davies, J. E. D.; McNicol, D. D. *Structural Aspects of Inclusion Compounds formed by Organic Host lattices*; Academic Press Inc.: London, 1984; Vol. 2.

(5) Wöhler, F. Ueber einige Verbindungen aus der Chinonreihe. *Justus Liebigs Ann. Chem.* **1849**, *69*, 294−300.

(6) Coupan, R.; Torré, J.-P.; Dicharry, C.; Hemati, M.; Plantier, F. Kinetics of CO_2 Capture by Hydroquinone Clathrates. *Ind. Eng. Chem. Res.* **2018**, *57*, 8172−8182.

(7) McAdie, H. G. Thermal Decomposition of Molecular Complexes: II. β-Quinol Clathrates. *Can. J. Chem.* **1963**, *41*, 2137−2143.

(8) Torré, J.P.; Coupan, R.; Chabod, M.; Péré, E.; Labat, S.; Khoukh, A.; Brown, R.; Sotiropoulos, J.-M.; Gornitzka, H. CO_2−Hydroquinone clathrate: Synthesis, Purification, Characterization and Crystal Structure. *Cryst. Growth Des.* **2016**, *16*, 5330−5338.

(9) Lee, Y. J.; Han, K. W.; Jang, J. S.; Jeon, T. I.; Park, J.; Kawamura, T.; Yamamoto, Y.; Sugahara, T.; Vogt, T.; Lee, J. W.; et al. Selective CO_2 Trapping in Guest free Hydroquinone Clathrate Prepared by Gas Phase Synthesis. *ChemPhysChem* **2011**, *12*, 1056−1059.

(10) Coupan, R.; Péré, E.; Dicharry, C.; Torré, J.-P. New Insights on Gas Hydroquinone Clathrates Using in Situ Raman Spectroscopy: Formation/Dissociation Mechanisms, Kinetics, and Capture Selectivity. *J. Phys. Chem. A* **2017**, *121*, 5450−5458.

(11) Chleck, D. J.; Ziegler, C. A. The Preparation and Some Properties of Radioactive Quinol-Krypton Clathrate Compounds. *Int. J. Appl. Radiat. Isot.* **1959**, *7*, 141−144.

(12) Hayes, D. G.; Bengtsson, Y. C.; Van Alstine, J. M.; Setterwall, F. Urea Complexation for the Rapid, Ecologically Responsible Fractionation of Fatty Acids from Seed Oil. *J. Am. Oil Chem. Soc.* **1998**, *75*, 1403−1409.

(13) Han, K. W.; Lee, Y.-J.; Jang, J. S.; Jeon, T.-I.; Park, J.; Kawamura, T.; Yamamoto, Y.; Sugahara, T.; Vogt, T.; Lee, J.-W.; et al. Fast and Reversible Hydrogen Storage in Channel Cages of Hydroquinone Clathrate. *Chem. Phys. Lett.* **2012**, *546*, 120−124.

(14) Rozsa, V. F.; Strobel, T. A. Triple Guest Occupancy and Negative Compressibility in Hydrogen-Loaded β-Hydroquinone Clathrate. *J. Phys. Chem. Lett.* **2014**, *5*, 1880−1884.

(15) Lee, J.-W.; Poudel, J.; Cha, M.; Yoon, S. J.; Yoon, J.-H. Highly Selective CO_2 Extraction from a Mixture of CO2 and H2 Gases Using Hydroquinone Clathrates. *Energy Fuels* **2016**, *30*, 7604−7609.

(16) Lee, J.-W.; Dotel, P.; Park, J.; Yoon, J.-H. Separation of CO_2 from Flue Gases using Hydroquinone Clathrate Compounds. *Korean J. Chem. Eng.* **2015**, *12*, 2507−2511.

(17) Coupan, R.; Dicharry, C.; Torré, J.-P. (2018). Hydroquinone Clathrate Based Gas Separation (HCBGS): Application to the CO_2/CH_4 Gas Mixture. *Fuel* **2018**, *226*, 137−147.

(18) Powell, H. M. J. The Structure of molecular compounds. Part IV: Clathrate Compounds. *J. Chem. Soc.* **1948**, 61−73.

(19) Conde, M. M.; Torré, J. P.; Miqueu, C. Revisiting the Thermodynamic Modelling of Type I Gas-Hydroquinone Clathrates. *Phys. Chem. Chem. Phys.* **2016**, *18*, 10018−10027.

(20) Coupan, R.; Chabod, M.; Dicharry, C.; Diaz, J.; Miqueu, C.; Torré, J.-P. Experimental Determination of Phase Equilibria and Occupancies for CO_2, CH_4, and N_2 Hydroquinone-Clathrates. *J. Chem. Eng. Data* **2016**, *61*, 2565−2572.

(21) Coupan, R.; Conde, M. M.; Miqueu, C.; Dicharry, C.; Torré, J.-P. Phase equilibrium properties of CO_2/CH_4 mixed gas hydroquinone clathrates: experimental data and model predictions. *J. Chem. Therm.* **2018**, *116*, 230−234.

(22) Lee, J.-W.; Yoon, J.-H. Preferential Occupation of CO_2 Molecules in Hydroquinone Clathrates Formed from CO_2/N_2 Gas Mixtures. *J. Phys. Chem. C* **2011**, *115*, 22647−22651.
(23) Park, J.-W.; An, S.; Seo, Y.; Kim, B.-S.; Yoon, J.-H. Temperature-Dependent Release of Guest Molecules and Structural Transformation of Hydroquinone Clathrates. *J. Phys. Chem. C* **2013**, *117*, 7623−7627.
(24) Coupan, R.; Péré, E.; Dicharry, C.; Plantier, F.; Diaz, J.; Khoukh, A.; Allouche, J.; Labat, S.; Pellerin, V.; Grenet, J.-P.; et al. A Characterization Study of CO_2, CH_4, and CO_2/CH_4 Hydroquinone Clathrates Formed by Gas-Solid Reaction. *J. Phys. Chem. C* **2017**, *121*, 22883−22894.
(25) Lee, J.-W.; Kang, S.-P.; Yoon, J.-H. Competing Occupation of Guest Molecules in Hydroquinone formed from binary C_2H_4 and CH_4 gas mixtures. *J. Phys. Chem. C* **2014**, *118*, 7705−7709.
(26) Lee, J.-W.; Kang, S.-P.; Yoon, J.-H. Highly Selective Enclathration of Ethylene from Gas Mixtures. *J. Phys. Chem. C* **2014**, *118*, 6059−6063.
(27) Sum, A. K.; Wu, D. T.; Yasuoka, K. Energy Science of Clathrate Hydrates: Simulation-Based Advances. *MRS Bull.* **2011**, *36*, 205−210.
(28) Barnes, B. C.; Sum, A. K. Advances in Molecular Simulations of Clathrate Hydrates. *Curr. Opin. Chem. Eng.* **2013**, *2*, 184−190.
(29) Dang, L. X.; Pettitt, B. M. A Theoretical Study of the Inclusion Complexes of β-Quinol. *J. Chem. Phys.* **1988**, *89*, 968−974.
(30) Dang, L. X.; Pettitt, B. M. Thermodynamics of Diatomic Guests in β-Quinol Clathrates. *J. Phys. Chem.* **1989**, *93*, 3794−3799.
(31) Santikary, P.; Yashonath, S.; Rao, C. Molecular Dynamics Simulation of Clathrates: Noble Gases in the Cages of β-Hydroquinone. *Chem. Phys. Lett.* **1992**, *192*, 390−394.
(32) Daschbach, J. L.; Chang, T.-M.; Corrales, L. R.; Dang, L. X.; McGrail, P. Molecular Mechanisms of Hydrogen-Loaded β-Hydroquinone Clathrate. *J. Phys. Chem. B* **2006**, *110*, 17291−17295.
(33) Pérez-Rodríguez, M.; Otero-Fernández, J.; Comesaña, A.; Fernández-Fernández, Á. M.; Piñeiro, M. M. Simulation of Capture and Release Processes of Hydrogen by β-Hydroquinone Clathrate. *ACS Omega* **2018**, *3*, 18771−18782.
(34) Nemkevich, A.; Spackman, M. A.; Corry, B. Mechanism of Concerted Hydrogen Bond Reorientation in Clathrates of Dianin's Compound and Hydroquinone. *J. Am. Chem. Soc.* **2011**, *133*, 18880−18888.
(35) Zubkus, V. E.; Shamovsky, I. L.; Tornau, E. E. Computer-Simulation Studies of β-Quinol Clathrate with Various Gases. Molecular Interactions and Crystal Structure. *J. Chem. Phys.* **1992**, *97*, 8617−8627.
(36) Zubkus, V. E.; Shamovsky, I. L. Molecular Interactions, Structure and Stability of β-Quinol Clathrate. *Chem. Phys. Lett.* **1992**, *195*, 135−143.
(37) Comesaña, A.; Pérez-Rodríguez, M.; Fernández, A. M.; Piñeiro, M. M. A Description of Hydroquinone Clathrates Using Molecular Dynamics: Molecular Model and Crystalline Structure for CH_4 and CO_2 Guests. *J. Chem. Phys.* **2018**, *148*, No. 244502.
(38) Li, X.; Chen, Q. Y.; Wang, J. Solubility of Hydroquinone in Different Solvents from 276.65 K to 345.10 K. *J. Chem. Eng. Data* **2006**, *51*, 127−129.
(39) Mercury 3.10.3 (Build 224359), Copyright CCDC 2001−2018. http://www.ccdc.cam.ac.uk/mercury/.
(40) Bekker, H.; Berendsen, H.; Dijkstra, E.; Achterop, S.; Vondrumen, R.; Vanderspoel, D.; Sijbers, A.; Keegstra, H.; Renardus, M. GROMACS: A Parallel Computer for Molecular Dynamics Simulations. In *Physics Computing 92*; DeGroot, R., Nadrchal, J., Eds.; World Scientific Publishing, 1993; pp 252−256.
(41) Berendsen, H. J. C.; van der Spoel, D.; van Drunen, R. ROMACS: A Message-Passing Parallel Molecular Dynamics Implementation. *Comput. Phys. Commun.* **1995**, *91*, 43−56.
(42) Jorgensen, W. L.; Maxwell, D. S.; Tirado-Rives, J. Development and Testing of the OPLS All-Atom Force Field on Conformational Energetics and Properties of Organic Liquids. *J. Am. Chem. Soc.* **1996**, *118*, 11225−11236.
(43) Becke, A. D. Density-Functional Thermochemistry. III. The Role of Exact Exchange. *J. Chem. Phys.* **1993**, *98*, 5648−5652.
(44) Lee, C.; Yang, W.; Parr, R. G. Development of the Colle-Salvetti Correlation-Energy Formula into a Functional of the Electron Density. *Phys. Rev. B* **1988**, *37*, 785−789.
(45) Frisch, M. J.; Trucks, G. W.; Schlegel, H. B.; Scuseria, G. E.; Robb, M. A.; Cheeseman, J. R.; Scalmani, G.; Barone, V.; Mennucci, B.; Petersson, G. A.;et al. *Gaussian 09*, revision D.01; Gaussian, Inc.: Wallingford, CT, 2009.
(46) Breneman, C. M.; Wiberg, K. B. Determining Atom-Centered Monopoles from Molecular Electrostatic Potentials. The Need for High Sampling Density in Formamide Conformational Analysis. *J. Comput. Chem.* **1990**, *11*, 361−373.
(47) Bussi, G.; Donadio, D.; Parrinello, M. Canonical Sampling Through Velocity Rescaling. *J. Chem. Phys.* **2007**, *126*, No. 014101.
(48) Darden, T.; York, D.; Pedersen, L. Particle Mesh Ewald: An N·log(N) Method for Ewald Sums in Large Systems. *J. Chem. Phys.* **1993**, *98*, 10089−10092.
(49) Essmann, U.; Perera, L.; Berkowitz, M. L.; Darden, T.; Lee, H.; Pedersen, L. G. A Smooth Particle Mesh Ewald Method. *J. Chem. Phys.* **1995**, *103*, 8577−8593.
(50) Good, R. J.; Hope, C. J. Test of Combining Rules for Intermolecular Distances. Potential Function Constants from Second Virial Coefficients. *J. Chem. Phys.* **1971**, *55*, 111−116.
(51) Turner, M. J.; McKinnon, J. J.; Jayatilaka, D.; Spackman, M. A. Visualisation and Characterisation of Voids in Crystalline Materials. *CrystEngComm* **2011**, *13*, 1804−1813.
(52) Johnstone, R. D. L.; Lennie, A. R.; Parker, S. F.; Parsons, S.; Pidcock, E.; Richardson, P. R.; Warren, J. E.; Wood, P. A. High-Pressure Polymorphism in Salicylamide. *CrystEngComm* **2010**, *12*, 1065−1078.
(53) Moggach, S. A.; Görbitz, C. H.; Warren, J. E. The Effect of Pressure on the Porous Peptide L-alanyl-L-valine. *CrystEngComm* **2010**, *12*, 2322−2324.
(54) Fabbiani, F. P. A.; Levendis, D. C.; Buth, G.; Kuhs, W. F.; Shankland, N.; Sowa, H. Searching for Novel Crystal Forms by in situ High-Pressure Crystallisation: the Example of Gabapentin Heptahydrate. *CrystEngComm* **2010**, *12*, 2354−2360.
(55) Mohamed, S.; Karothu, D. P.; Naumov, P. Using Crystal Structure Prediction to Rationalize the Hydration Propensities of Substituted Adamantane Hydrochloride Salts. *Acta Crystallogr., Sect. B: Struct. Sci., Cryst. Eng. Mater.* **2016**, *72*, 551−561.
(56) Linga, P.; Kumar, R.; Englezos, P. The Clathrate Hydrate Process for Post and Pre-Combustion Capture of Carbon Dioxide. *J. Hazard. Mater.* **2007**, *149*, 625−629.

DOI: 10.1021/acs.jpcc.9b04081

SUPPORTING INFORMATION

Insights into the Crystal Structure and Clathration Selectivity of Organic Clathrates formed with Hydroquinone and (CO_2 + CH_4) Gas Mixtures

*Jean-Philippe TORRÉ [1, *], Heinz GORNITZKA [2], Romuald COUPAN [3], Christophe DICHARRY [4]*

Martín PÉREZ-RODRÍGUEZ [5], Antonio COMESAÑA [5], Manuel M. PIÑEIRO [5]

[1]. Laboratoire de Génie Chimique, Université de Toulouse, CNRS, INPT, UPS, Toulouse, France.

[2]. Laboratoire de Chimie de Coordination LCC-CNRS, Université de Toulouse, CNRS, UPS, Toulouse, France.

[3]. Total Research & Technology Feluy, Zone Industrielle Feluy C, B-7181 Seneffe, Belgium.

[4]. CNRS/TOTAL/UNIV PAU & PAYS ADOUR/E2S UPPA, Laboratoire des Fluides Complexes et leurs Réservoirs-IPRA, UMR5150 – avenue de l'Université, 64000 Pau, France.

[5]. Departamento de Física Aplicada, Facultade de Ciencias, Universidade de Vigo, 36310, Spain.

Table S1. Analytical techniques and methods used in this study.

Method	Details
GC	The gas composition at the end of the synthesis is obtained by gas chromatography (**GC**). The analysis is performed using a gas chromatograph (GC Agilent, model 7820A) equipped with a high-pressure sampling system, a 30-m capillary column (model HP-PLOT-Q) with an inner diameter of 0.32 mm (comprising a stationary phase of polystyrene/di-vinylbenzene coating, 20 µm thick), and a thermal conductivity detector. Hydrogen, supplied by a hydrogen generator (model NMH2), is used as a carrier gas. The GC is calibrated with different commercial CO_2/CH_4 gas mixtures. The method allows quantitative measurements with a relative uncertainty of 0.3%, and retention times for CH_4 and CO_2 of 0.64 ± 0.05 and 0.80 ± 0.05 minutes respectively.
XRD	The X-Ray Diffraction (**XRD**) analysis were performed using oil-coated shock-cooled crystals on a Bruker-AXS APEX II diffractometer with MoKa radiation (λ = 0.71073 Å). The crystal structures were solved by direct methods [Sheldrick, G. M. *Acta Cryst*. **2008**, *A64*, 112–122] and all non-hydrogen atoms were refined anisotropically using the least-squares method on F^2 [Sheldrick, G. M. *Acta Cryst.* **2015**, *C71*, 3-8].

Table S2. Information concerning the materials used for this study. The products were used without further purification.

Product	Abbreviation	Purity (mole %)	Supplier
Hydroquinone	HQ	99.5 %	Acros Organics
Ethanol absolute	EtOH	>99%	Sigma Aldrich
Carbon dioxide	CO_2	> 99.995 %	Linde gas
Methane	CH_4	> 99.995 %	Linde gas
Gas mixtures	CO_2/CH_4	> 99.995 %	Linde gas

Table S3. Summary of the experimental data obtained in this study. Variables: CO_2 molar fraction in the gas used for the synthesis (y^{CO2}_{init}), CO_2 molar fraction in the gas phase in equilibrium with the solid phase measured at the end of the experiment (y^{CO2}), *A* and *B* parameters of the clathrate formula ($A\ CO_2 - B\ CH_4 - 3HQ$), crystal lattice parameters (*a, b, c*), tilt angle of the HQ molecule in the crystal (α), volume of the unit cell (V_{uc}), total occupancy of the guests in the clathrate (χ), CO_2 molar fraction in the crystal (x^{CO2}), ratio of the CO_2 and CH_4 molar fractions in the crystal ($S^{CO2/CH4}$), and separation factor ($S.F.^{CO2:CH4}$). The uncertainty ± Δ is within the 95% confidence interval of the mean, under the assumption of normality, estimated from 3 repeat experiments (CDCC 1913199-1913201).

Variable	y^{CO2}_{init}	y^{CO2}	***A***	***B***	***a, b***	***c***	***α***	V_{uc}	***χ***	x^{CO2}	$S^{CO2/CH4}$	$S.F.^{CO2/CH4}$
unit	-	-	-	-	*Å*	*Å*	*deg*	*Å*^{3}	-	-	-	-
± Δ	0.008	0.032	0.06	0.06	0.042	0.014	0.4	4	0.12	0.03	0.4	0.6
CDCC-1913196	0.000	0.000	0.00	0.81	16.562	5.405	40.2	1284	0.81	0.00	0.0	-
CDCC-1913197	0.106	0.087	0.19	0.65	16.529	5.430	40.7	1285	0.84	0.23	0.3	3.1
CDCC-1913198	0.255	0.243	0.39	0.33	16.416	5.496	41.7	1283	0.72	0.54	1.2	3.7
CDCC-1913199	0.502	0.483	0.58	0.23	16.321	5.580	42.9	1287	0.81	0.72	2.5	2.7
CDCC-1913200	0.497	0.457	0.59	0.23	16.325	5.573	42.8	1286	0.82	0.72	2.6	3.0
CDCC-1913201	0.503	0.470	0.54	0.19	16.352	5.569	42.6	1289	0.73	0.74	2.8	3.2
CDCC-1913202	0.640	0.596	0.71	0.16	16.265	5.623	43.4	1288	0.87	0.82	4.4	3.0
CDCC-1913203	0.742	0.691	0.75	0.08	16.235	5.644	43.8	1288	0.83	0.90	9.4	4.2
CDCC-1913204	1.000	1.000	0.83	0.00	16.189	5.688	44.3	1291	0.83	1.00	-	-

Table S4. Statistical analysis with the data of **Figure 6** (distribution of the tilt angle (α) of the HQ molecule in the clathrate structure for three values of CO_2 molar fractions in the solid). Number of observations: 576. The Kolmogorov-Smirnov test was used to evaluate whether scores were likely to follow normal distribution in the populations.

	Min	Max	Average	Std deviation	*p-value* (Kolmogorov-Smirnov test) [(1)]
x= 0	35.495	39.411	37.427	0.686	0.875
x=0.5	35.767	42.187	39.466	1.099	0.608
x=1	40.891	45.206	43.067	0.698	0.985

[(1)] if the *p-value* is > 0.05, the assumption of normality cannot be rejected (i.e. the data follow normal distribution).